Biochimica et Biophysica Acta 1843 (2014) 2448–2460

Contents lists available at ScienceDirect

Biochimica et Biophysica Acta

journal homepage: www.elsevier.com/locate/bbamcr

Thioredoxin-interacting protein mediates NALP3 inflammasome activation in podocytes during diabetic nephropathy

Pan Gao [a], Xian-Fang Meng [b], Hua Su [a], Fang-Fang He [a], Shan Chen [a], Hui Tang [a], Xiu-Juan Tian [a], Di Fan [a], Yu-Mei Wang [a], Jian-She Liu [a], Zhong-Hua Zhu [a], Chun Zhang [a,*]

[a] Department of Nephrology, Union Hospital, Tongji Medical College, Huazhong University of Science and Technology, Wuhan 430022, China
[b] Department of Neurobiology, Tongji Medical College, Huazhong University of Science and Technology, Wuhan 430030, China

ARTICLE INFO

Article history:
Received 27 January 2014
Received in revised form 1 July 2014
Accepted 2 July 2014
Available online 10 July 2014

Keywords:
TXNIP
NALP3 inflammasome
Diabetic nephropathy
Podocyte

ABSTRACT

Numerous studies have shown that the NALP3 inflammasome plays an important role in various immune and inflammatory diseases. However, whether the NALP3 inflammasome is involved in the pathogenesis of diabetic nephropathy (DN) is unclear. In our study, we confirmed that high glucose (HG) concentrations induced NALP3 inflammasome activation both in vivo and in vitro. Blocking NALP3 inflammasome activation by NALP3/ASC shRNA and caspase-1 inhibition prevented IL-1β production and eventually attenuated podocyte and glomerular injury under HG conditions. We also found that thioredoxin (TRX)-interacting protein (TXNIP), which is a pro-oxidative stress and pro-inflammatory factor, activated NALP3 inflammasome by interacting with NALP3 in HG-exposed podocytes. Knocking down TXNIP impeded NALP3 inflammasome activation and alleviated podocyte injury caused by HG. In summary, the NALP3 inflammasome mediates podocyte and glomerular injury in DN, moreover, TXNIP participates in the formation and activation of the NALP3 inflammasome in podocytes during DN, which represents a novel mechanism of podocyte and glomerular injury under diabetic conditions.

1. Introduction

Diabetic nephropathy (DN) is the most common chronic microvascular complication of diabetes. Due to its high morbidity and mortality [1], it has become a primary reason for end stage renal disease (ESRD) in patients and a major global public health problem [2–4]. Therefore, understanding the pathogenesis is critical for its prevention and treatment. Podocytes are considered to be the primary cause of the onset and progression of DN [5–8]. For example, the loss of podocytes was observed in patients with early and late DN [9,10]. However, the early pathogenic mechanisms of DN are not fully understood yet.

Immunity and inflammation are responsible for the occurrence and progression of glomerular diseases, particularly podocyte injury and glomerulosclerosis. The inflammasome is defined as an intracellular organelle governing immune and inflammatory processes [11]. Inflammasomes are a large family, among which the NALP3 inflammasome is a typical member in mammalian cells. The NALP3 inflammasome is composed of NALP3 (NACHT, LRR and PYD domains-containing protein 3), ASC (apoptosis-associated speck like protein) and caspase-1. NALP3 can recruit caspase-1 via adapter molecular ASC to form a proteolytic complex "NALP3 inflammasome" [12,13] and each component is essential to inflammasome activation [14].

ASC is necessary for caspase-1 activation and subsequent mature interleukin-1β (IL-1β) secretion when responding to various danger-associated molecular patterns (DAMPs) or pathogen-associated molecular patterns (PAMPs) [11,13,15,16]. IL-1β is primarily produced by podocytes in the glomeruli [17], and importantly participates in kidney injury and repair [18]. In podocytes, active caspase-1 is indispensable for cleaving the inactive pro-IL-1β into its active form [19]. Recently, the NALP3 inflammasome was identified as a possible therapeutic target in patients with progressive CKD [20]. Additionally, the NALP3 agonist biglycan, the IL-1 receptor, and cytokines such as IL-1β can all accelerate renal inflammation and fibrosis [21,22]. Yet, it remains to be explored whether the NALP3 inflammasome is involved in podocyte injury of DN. It is also necessary to determine the early regulatory mechanisms of the NALP3 inflammasome activation and subsequent podocyte damage.

Recently, it has been shown that NALP3 can interact with thioredoxin (TRX)-interacting protein (TXNIP), which is related to insulin resistance, and that TXNIP deletion impedes NALP3 inflammasome activation and subsequent IL-1β production in immune cells [23,24]. The expression of TXNIP mRNA and protein is highest in the glomeruli and distal nephron of normal human and rat kidney, and knockdown of TXNIP decreases oxidative stress [25]. There is a wealth of evidence indicating that TXNIP is associated with glucose metabolism and diabetes [23,26–28]. However, it is still unknown that, whether TXNIP can mediate the activation of NALP3 inflammasome and ultimately cause podocyte injury in DN.

* Corresponding author.
E-mail address: drzhangchun@hust.edu.cn (C. Zhang).

http://dx.doi.org/10.1016/j.bbamcr.2014.07.001
0167-4889/

Our current study suggests that TXNIP mediates the NALP3 inflammasome activation, which plays a vital role in podocyte and glomerular inflammatory damage during DN.

2. Materials and methods

2.1. Animals

All experiments were performed according to the guidelines for use and care of laboratory animals of National Institutes of Health (NIH), and approved by the Animal Care and Use Committee (ACUC) of Tongji Medical College. Caspase-1 knockout (KO) mice were obtained from Jackson Laboratories (Bar Harbor, Maine, USA). Wide type (WT) mice and caspase-1 KO mice of eight-week-old, received a single intraperitoneal injection of streptozotocin (STZ, 150 mg/kg; Enzo Life Sciences, Ann Arbor, MI, USA). Eight-week-old control mice received only an injection of citrate buffer. Blood glucose levels were monitored weekly by glucometer readings. Only mice with stable glucose levels more than 16.7 mmol/l (95%) were included in the study. After 8 weeks of experimental diabetes, we placed all mice into metabolic cages and then collected urine samples after 24 h, before collecting blood samples and kidney tissues. Urinary albumin and creatinine measurements were performed by Auto-Chemistry Analyzer of DIRUI CS-400B (Changchun, Jilin, China).

2.2. Cell culture

An immortalized human podocyte cell line was cultured and maintained as described previously [29]. Briefly, cells were cultured in RPMI-1640 medium supplemented with both 10% fetal bovine serum (FBS) and 100 U/ml penicillin-streptomycin in humidified 5% CO_2 incubator and firstly incubated at 33 °C. After the cells reached at 70% confluence, they were incubated at 37 °C for 2 weeks to allow differentiation before any experimental manipulations. When differentiated cells had grown up to 75% confluence, they were transferred to 2% FBS media for 12 h. These cells were exposed to media containing either normal glucose (as a control,5.6 mmol/l D-glucose) or high glucose (HG, 30 mmol/l D-glucose) for 12, 24 and 48 h. Moreover, osmotic pressure control was used by 24.4 mmol/l mannitol plus 5.6 mmol/l D-glucose.

2.3. NALP3 shRNA, ASC shRNA, and TXNIP siRNA

NALP3 shRNA and ASC shRNA were obtained from Genechem (Shanghai, China), and they were useful in silencing NALP3/ASC gene in podocytes. The scrambled shRNA (Genechem, Shanghai, China) was used as a control. Podocytes were synchronized for 12 h and then transiently transfected with NALP3/ASC shRNA or scrambled shRNA. To knock down TXNIP, we treated human podocytes with siRNA against human TXNIP coding region. The target sequences were 5′-AAGCCGTT AGGATCCTGGCTT-3′ for human siTXNIP and 5′-AATTCTCCGAACGTGT CACGT-3′ for scrambled siRNA (QIAGEN, Germantown, MD, USA). The transfection protocol was done by using lipofectamine 2000 (Invitrogen Corp., Carlsbad, CA, USA) according to the manufacturer's instruction. After 24 h, HG (30 mmol/l) was mixed into the medium for the corresponding time to conduct the following experiments.

2.4. Indirect immunofluorescent staining and confocal microscopy

To localize inflammasome components with podocyte in the mouse kidney, frozen tissue slides were used to perform double-immunofluorescent staining. After fixation for 15 min, the slides were permeabilized with 0.3% Triton X-100 in PBS for 5 min, blocked with 5% donkey serum for 30 min, and then incubated overnight at 4 °C with goat anti-synaptopodin antibody (1:40; Santa Cruz Biotechnology, Santa Cruz, CA, USA) and rabbit anti-NALP3 (1:100; Protein Tech Group, Chicago, IL), goat anti-synaptopodin antibody (1:40; Santa Cruz Biotechnology, Santa Cruz, CA, USA) and rabbit anti-ASC antibody (1:50; Enzo, Plymouth Meeting, PA, USA), or goat anti-synaptopodin antibody (1:40; Santa Cruz Biotechnology, Santa Cruz, CA, USA) and mouse anti-caspase-1 antibody (1:50; Santa Cruz Biotechnology, Santa Cruz, CA, USA). Synaptopodin was used as the marker of podocyte. In additional experiments, tissue slides were probed with mouse anti-TXNIP antibody (1:100; MBL International Co, Woburn, MA, USA) together with goat anti-synaptopodin antibody (1:40; Santa Cruz Biotechnology, Santa Cruz, CA, USA) to show the localization of TXNIP and podocytes. After washing, these slides were incubated with Alexa-488-labeled or Alexa-647-labeled secondary antibodies for 1 h at room temperature. After being stained with DAPI, the slides were examined by confocal laser scanning microscopy (Fluoview FV1000, Olympus, Japan). Separate staining of Alexa-488-labeled or Alexa-647-labeled secondary antibody alone was used as negative control. No visible fluorescence was detected under these conditions, which indicates the specific staining of above antibodies. The colocalization was analyzed by the Image Pro Plus 6.0 software (Media Cybernetics, Bethesda, MD, USA).

2.5. Human renal biopsy samples and immunohistochemical studies

Renal biopsy was performed routinely. The patient samples were obtained from the Department of Nephrology of Union Hospital, Tongji Medical College, Huazhong University of Science and Technology. Control samples were obtained from the healthy kidney poles of individuals who underwent nephrectomy due to tumor, without diabetes or any other renal diseases. All the procedures were approved by the Ethics Committee of Tongji Medical College, Huazhong University of Science and Technology.

Paraffin-embedded kidney tissue sections were prepared at 4 μm thicknesses, and stained with antibodies to NALP3, ASC, or caspase-1 according to immunohistochemistry procedure. After staining, randomly choosing glomerular cross sections to calculate positively stained area using Image Pro Plus 6.0 software (Media Cybernetics, Bethesda, MD, USA). The data were exhibited as integrated optical density (IOD).

2.6. Western blot analysis

Western blot analyses were performed as we described previously [19]. In brief, proteins from mouse glomeruli or cultured human podocytes were extracted with RIPA Lysis Buffer (Beyotime, Jiangsu, China). After boiling for 5 min at 95 °C in 5× loading buffer, 30 μg of mouse glomeruli protein or 80 μg of cultured human podocyte proteins were subjected to SDS-PAGE, transferred to PVDF membrane and blocked for 1 h. The membranes were incubated overnight at 4 °C with the following primary antibodies of rabbit anti-NALP3 antibody (1:1000; Protein Tech Group, Chicago, IL), rabbit anti-ASC antibody (1:50; Enzo, Plymouth Meeting, PA, USA), rabbit anti-caspase-1 antibody (1:100; Santa Cruz Biotechnology, Santa Cruz, CA, USA), mouse anti-desmin antibody (1:1000; Protein Tech Group, Chicago, IL), rabbit anti-synaptopodin antibody (1:1000; Protein Tech Group, Chicago, IL), mouse anti-TXNIP antibody (1:1000; MBL, International Co, Woburn, MA, USA) or mouse anti-β-actin antibody (1:10000; Santa Cruz Biotechnology, Santa Cruz, CA, USA). After washing, the membranes were incubated with horseradish peroxidase-labeled IgG (1:10000) for 1 h at room temperature. The immunoreactive bands were detected by chemiluminescence methods and visualized on Kodak Omat X-ray films. Densitometric analysis of the images obtained from X-ray films was performed using the Image J software (NIH, Bethesda, MD, USA).

2.7. Caspase-1 activation detection

Caspase-1 activity was detected by a commercial kit (Biovision, Mountain View, CA, USA), which was used to represent the activation of NALP3 inflammasome. The data were calculated as the fold changes compared to control cells.

2.8. Activity of caspase-1 (green FLICA caspase-1 detection kit) in DN animals

This detection kit was obtained from Immunochemistry Technologies (Bloomington, MN, USA). After sample preparation, staining procedure was conducted according to the instruction described by the manufacturer.

2.9. Direct immunofluorescent staining of F-actin

To determine whether HG-induced NALP3 inflammasome activation could result in cytoskeleton changes of podocytes, podocytes were pretreated with caspase-1 inhibitor Z-YVAD-FMK (Z-YVAD; 10 μmol/l; Biovision, Mountain View, CA, USA) or transfected with NALP3/ASC shRNA or scrambled shRNA, TXNIP siRNA or scrambled siRNA, and then exposed to HG (30 mmol/l) for 48 h. The cells were fixed in 4% paraformaldehyde for 15 min at room temperature after washing, permeabilized for 5 min with 0.1% Triton X-100 in PBS, and blocked for 30 min with 5% BSA. F-actin was incubated with rhodamine–phalloidin (Invitrogen Corp., Carlsbad, CA, USA) for 15 min at room temperature. The slides were examined by confocal laser scanning microscopy. The cells with distinct F-actin fibers were counted as we described previously [30]. Scoring was obtained from 100 podocytes on each slide in different groups.

2.10. Transmission electron microscopy (TEM)

For detection of ultrastructural changes of podocytes, tissue samples were fixed with 3% glutaraldehyde in 0.1 mol/l phosphate buffer overnight. All samples were sent to Ultrastructural Pathology Center of Tongji Medical College for TEM examination.

2.11. Light microscopy

To observe renal morphology by light microscopy, the experimental procedures and specific scoring method were performed as we described previously [31].

2.12. ELISA for IL-1β in podocytes

After being transfected with ASC/NALP3 shRNA/scrambled shRNA; TXNIP siRNA/scrambled siRNA, or pretreated with caspase-1 inhibitor (Z-YVAD), podocytes were incubated with HG (30 mmol/l) for 48 h. The IL-1β production in supernatant was measured by ELISA assay according to the protocol described by the manufacturer (R&D Systems, Minneapolis, MN, USA).

2.13. TRX activity

Thioredoxin Reductase Colorimetric Assay Kit was obtained from Cayman Chemical Company. TRX activity was measured by the insulin disulfide reduction assay as described by the manufacturer.

2.14. Statistical analysis

All of the values are expressed as mean ± SEM. Significant differences among multiple groups were examined using ANOVA followed by a Student–Newman–Keuls post hoc test. $\chi 2$ test was used for testing the significance of ratio and percentage data. $P < 0.05$ was considered statistically significant.

3. Results

3.1. The NALP3 inflammasome is activated in podocytes of the glomeruli of both human DN specimens and DN mice

To determine whether NALP3 inflammasome is activated in podocytes of the glomeruli of DN, we first analyzed the expression of NALP3, ASC and caspase-1 in podocytes of the glomeruli of both human DN specimens and DN mice. By confocal microscopy we observed that the colocalization of NALP3 inflammasome components with synaptopodin increased in the glomeruli of both human DN specimens and DN mice comparing to their separate controls, even though the intensity of synaptopodin staining (podocyte marker) decreased in the glomeruli of DN mice (Fig. 1A–D). The enhanced expression of NALP3 inflammasome components in the glomeruli of DN mice was confirmed by immunohistochemistry (Fig. 1E, F).

3.2. HG induces NALP3 inflammasome activation in cultured human podocytes

Next, we evaluated whether HG directly activated NALP3 inflammasome in cultured human podocytes. It was found that HG increased NALP3, ASC, active caspase-1 and active IL-1β expression in a time-dependent manner by Western blot analyses in HG-treated podocytes (Fig. 2A, B). Mannitol was used to rule out the influence of osmotic pressure on NALP3 inflammasome (Data not presented). We also detected that both caspase-1 activity and IL-1β secretion (indicators of the NALP3 inflammasome activation) were upregulated in a time-dependent manner in HG-treated podocytes (Fig. 2C, D).

3.3. Suppression of the NALP3 inflammasome attenuates HG-induced NALP3 inflammasome activation and podocyte injury

As shown in Fig. 3A–D, the inhibition of both NALP3 and ASC by shRNA decreased HG-induced NALP3, ASC, active caspase-1 and active IL-1β expression in HG-treated podocytes. Inhibiting caspase-1 by Z-YVAD also impeded the pro-IL-1β cleavage. Also the interference above inhibited caspase-1 activity (Fig. 3E) and IL-1β secretion (Fig. 3F) in HG-exposed podocytes.

HG increased desmin expression and down-regulated synaptopodin in podocytes, which was consistent with previous publication [32]. However, pretreatment with ASC/NALP3 shRNA or Z-YVAD reversed the aforementioned effects (Fig. 4A–D). Besides, suppression of the NALP3 inflammasome prevented HG-induced loss and rearrangement of F-actin, a component, which is indispensable for refined structure and function of podocytes (Fig. 4E, F).

3.4. Caspase-1 deficiency suppresses NALP3 inflammasome function and alleviates glomerular and podocyte injury in DN mice

Under DN conditions, caspase-1 activity was enhanced in the glomeruli of WT mice, which was proved by Green FLICA Caspase-1 Detection Kit (Fig. 5A). The caspase-1 activity was absolutely inhibited in the glomeruli of caspase-1 KO mice under either normal or DN state. Also knocking down caspase-1 hampered the formation of active IL-1β in the glomerular lysate of DN mice (Fig. 5B, C).

We further investigated whether caspase-1 can participate in NALP3 inflammasome activation and glomerular/podocyte injury in DN mice. As was shown in Table 1, after STZ injection for 8 weeks, blood glucose significantly increased in both DN-WT mice and DN-KO mice compared to their respective controls, while there was no significant difference between them. Furthermore, although both DN-WT mice and DN-KO mice indicated a remarkable decrease in body weight and an obvious increase in kidney-to-body weight ratio compared with that in their separate control mice, knocking out caspase-1 in

DN mice obviously lowered kidney-to-body weight ratio. In addition, after STZ injection, urine albumin to creatinine ratio (UACR) increased 15-fold in both WT mice and KO mice, and caspase-1 deficiency did not alter albuminuria in the control mice, but reduced 30% UACR in the DN mice.

As shown in Fig. 6A, the pathological changes in the glomeruli of WT and KO mice were examined by PAS staining. It was found that the average glomeruli damage index (GDI) was higher in both DN-WT mice and DN-KO mice, while GDI in DN-KO mice was markedly lower compared to DN-WT mice (Fig. 6B). Then we studied the ultrastructure of podocytes under transmission electron microscopy (TEM). The normal structure of podocyte foot processes was observed in both Ctrl-WT mice and Ctrl-KO mice, whereas evident effacement of podocyte foot processes was discovered in DN-WT mice. Notably knocking down caspase-1 preserved the morphology of podocytes (Fig. 6C). Next, we assessed the effect of caspase-1 on the podocyte impairment in DN mice. By indirect immunofluorescent staining, we found that podocin and synaptopodin arranged along the glomerular capillary loop as a fine linear-like pattern in the glomeruli of Ctrl-WT mice and Ctrl-KO mice, but the staining of both podocin and synaptopodin presented a dramatic decrease in the glomeruli of DN-WT mice, which was reversed partly in DN-KO mice (Fig. 6D). Western blot analyses also reconfirmed that podocin and synaptopodin protein expression significantly decreased in the glomerular lysate of DN-WT mice; however, this phenomenon was not observed in the glomerular lysate of DN-KO mice (Fig. 6E, F).

3.5. TXNIP expression is upregulated in podocytes of DN mice

To understand the molecular mechanism of NALP3 inflammasome activation, we focused on TXNIP, which is a binding partner of reduced TRX and functions as a negative regulator of the TRX activity [33,34]. It

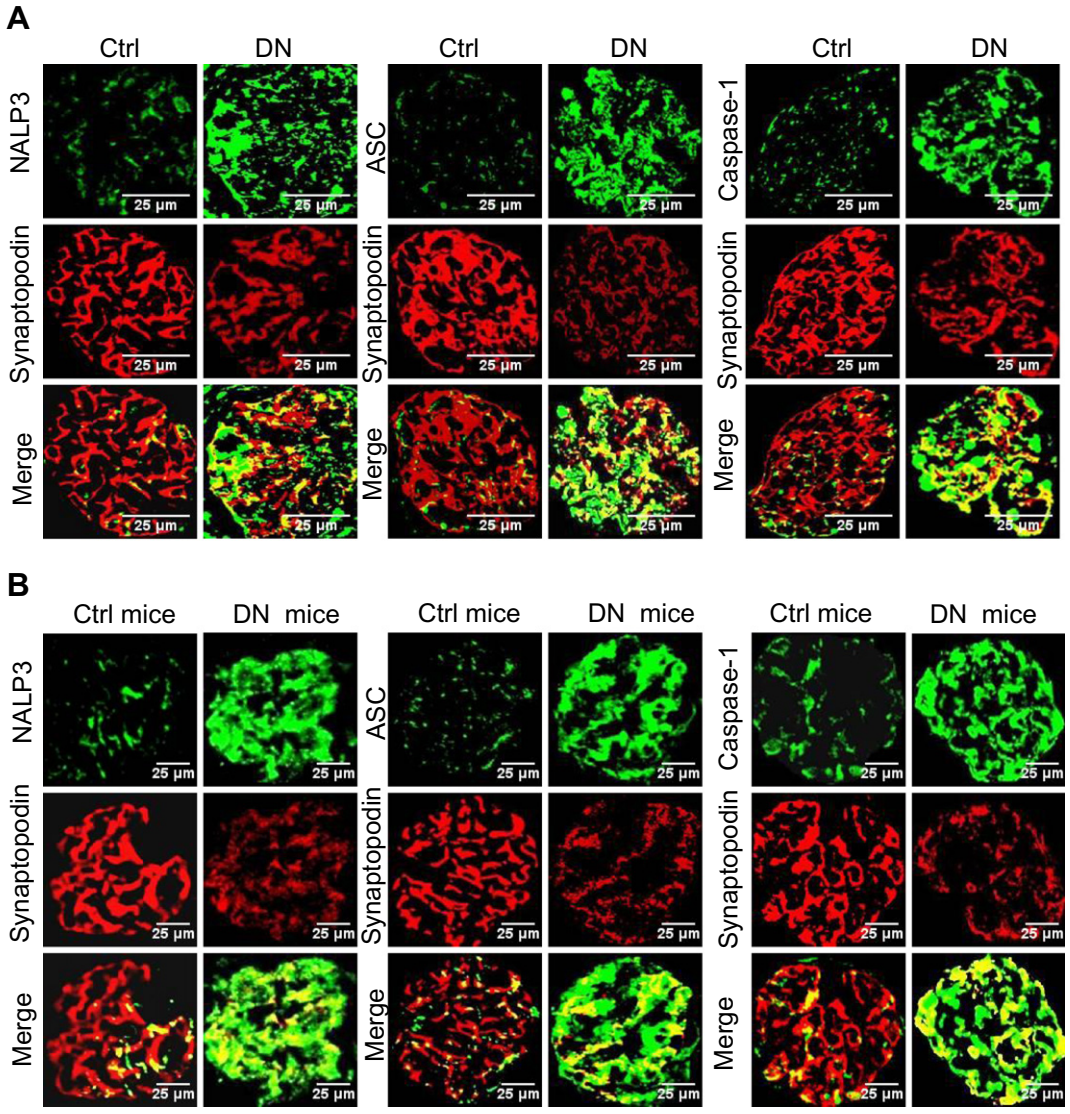

Fig. 1. The NALP3 inflammasome is activated in podocytes of the glomeruli of both human DN specimens and DN mice. A. Colocalization of NALP3 (green) with synaptopodin (red), ASC (green) with synaptopodin (red), and caspase-1 (green) with synaptopodin (red) in the glomeruli of both Ctrl and DN. B. Colocalization of NALP3 (green) with synaptopodin (red), ASC (green) with synaptopodin (red), and caspase-1 (green) with synaptopodin (red) in the glomeruli of both Ctrl mice and DN mice. C. Mean fluorescence intensity (MFI) of NALP3 with synaptopodin, ASC with synaptopodin, and caspase-1 with synaptopodin in the glomeruli of both Ctrl and DN ($n = 6$). Ctrl: human control samples; DN: human diabetic nephropathy specimens. $^{*, \#, \&}P < 0.05$ vs. Ctrl. D. MFI of NALP3 with synaptopodin, ASC with synaptopodin, and caspase-1 with synaptopodin in the glomeruli of both Ctrl mice and DN mice ($n = 6$). Ctrl mice: control mice; DN mice: diabetic nephropathy mice. $^{*, \#, \&}P < 0.05$ vs. Ctrl mice. E. Immunohistochemical staining of NALP3, ASC, and caspase-1 in the glomeruli of both Ctrl mice and DN mice. F. Summarized data of integrated optical density (IOD) ($n = 7$). Ctrl mice: control mice; DN mice: diabetic nephropathy mice. $^{*}P < 0.05$ vs. Ctrl mice.

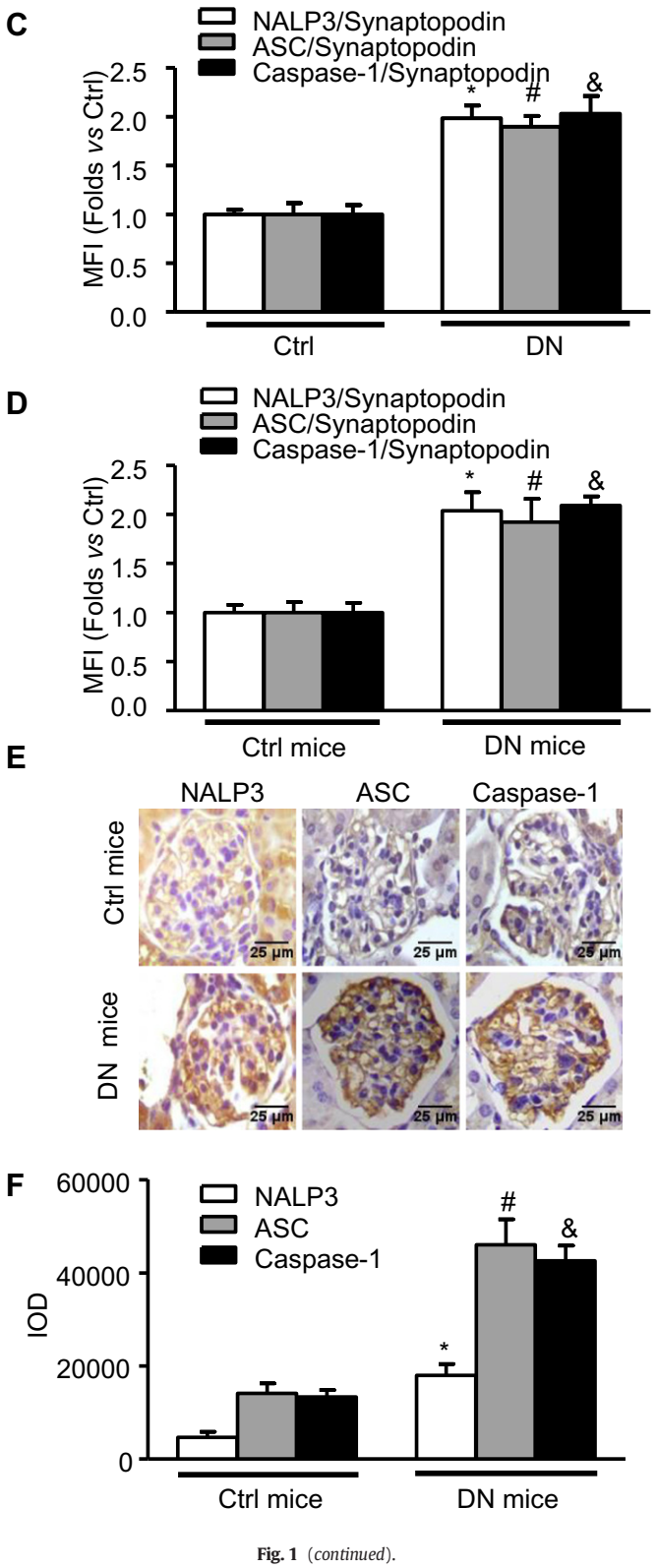

Fig. 1 (*continued*).

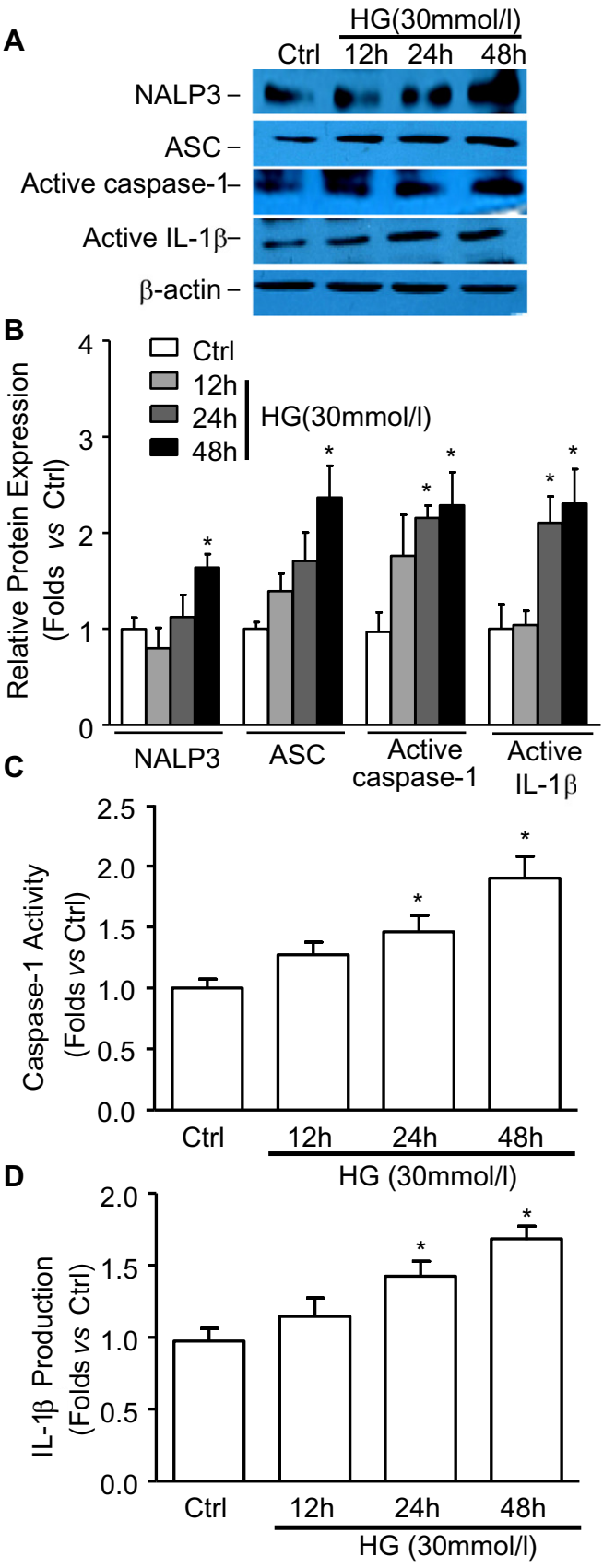

Fig. 2. HG induces NALP3 inflammasome activation in cultured human podocytes. A. Western-blotting gel documents showing the expression of NALP3, ASC, active caspase-1 and active IL-1β in cultured podocytes by HG. B. Protein expression of NALP3, ASC, active caspase-1 and active IL-1β in podocytes by HG (n = 6–8). C. Caspase-1 activity (n = 7). D. IL-1β production (n = 7). Ctrl: control; HG: high glucose; Veh:vehicle.*P < 0.05 vs. Ctrl.

was shown that TXNIP was increased in the glomerular lysate of DN mice (Fig. 7A, B). The upregulated TXNIP was found to mainly distribute in podocytes by confocal microscopy (Fig. 7C). Furthermore, in the glomerular lysate of DN mice, the interaction between TXNIP and NALP3 was strengthened as determined by co-immunoprecipitation (Fig. 7D).

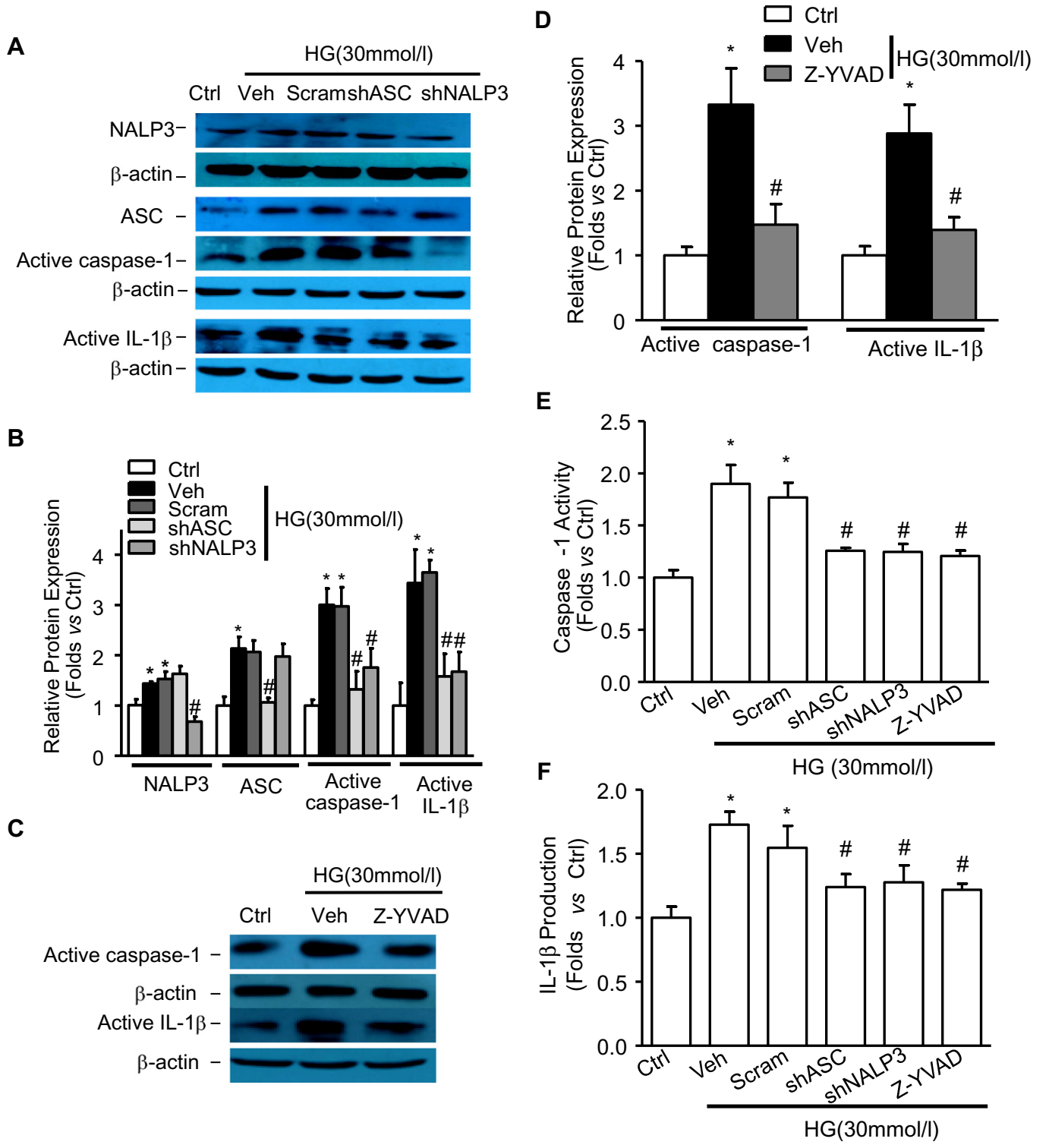

Fig. 3. Both NALP3/ASC gene silencing and caspase-1 inhibition suppress inflammasome activation and functional changes in HG-induced podocytes. A. Western blot analyses showing the expression of NALP3, ASC, active caspase-1 and active IL-1β in cultured human podocytes by ASC/NALP3 shRNA. B. Summarized data showing the protein expression of NALP3, ASC, active caspase-1 and active IL-1β by ASC/NALP3 shRNA (n = 5–7). C. Western blot analyses of the expression of active caspase-1 and active IL-1β by caspase-1 inhibitor Z-YVAD. D. Active caspase-1 and active IL-1β protein expression (n = 3–4). E. Caspase-1 activity (n = 6). F. IL-1β production (n = 6). Ctrl:control; HG:high glucose; Veh:vehicle; Scram:scrambled shRNA; shASC: ASC shRNA; shNALP3: NALP3 shRNA. $^{*}P < 0.05$ vs. Ctrl; $^{\#}P < 0.05$ vs. HG.

3.6. Silencing TXNIP mitigates the activation of NALP3 inflammasome

We revealed that HG exposure induced intensive expression of TXNIP in human podocytes within 48 h, which reached the peak at 48 h (Fig. 8A, B). What is more, TRX activity gradually time-dependently decreased within 48 h in HG-exposed podocytes (Fig. 8C). By coimmunoprecipitation assay, we observed the interaction between TXNIP and NALP3 in podocytes became gradually detectable as the HG exposure prolonged,

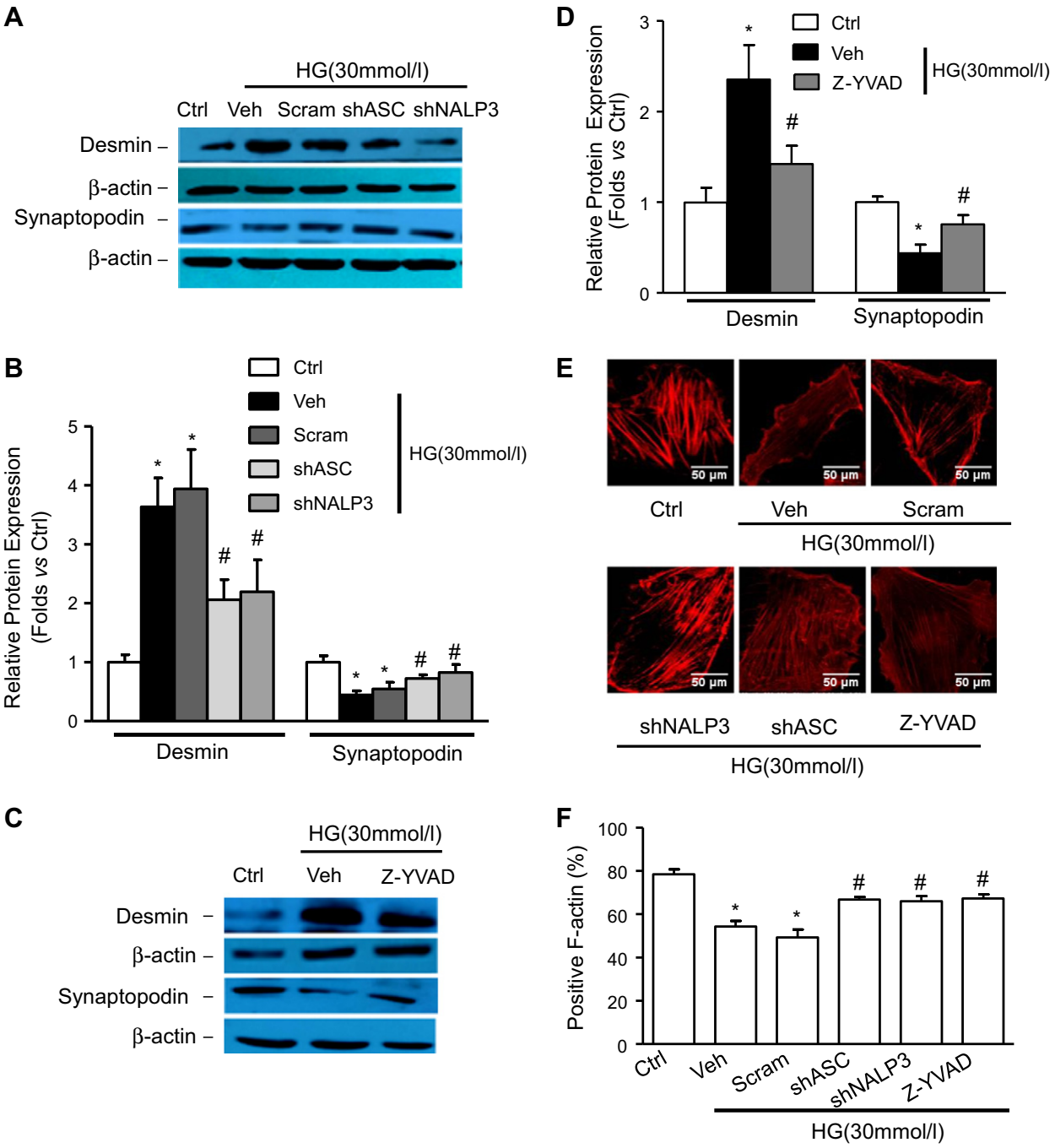

Fig. 4. Inhibition of NALP3 inflammasome attenuates HG-induced podocyte injury. A. Western blot analyses of both podocyte injury marker desmin and podocyte marker synaptopodin expression in cultured human podocytes by ASC/NALP3 shRNA. B. Protein expression of desmin and synaptopodin in cultured human podocytes (n = 7–9). C. Western blot analyses showing the effect of caspase-1 inhibitor Z-YVAD on the expression of desmin and synaptopodin in cultured human podocytes. D. Protein expression of desmin and synaptopodin in cultured human podocytes (n = 8–9). E. Microscopic images of F-actin by rhodamine–phalloidin staining. F. Summarized data from counting the cells with distinct, longitudinal F-actin fibers. Scoring was determined from 100 podocytes on each slide (n = 4). Ctrl:control; HG:high glucose; Veh:vehicle; Scram:scrambled shRNA; shASC: ASC shRNA; shNALP3: NALP3 shRNA. $^{*}P < 0.05$ vs. Ctrl; $^{\#}P < 0.05$ vs. HG.

which was more prominent after HG stimulation for 48 h. Inhibition of TXNIP by siRNA prevented the interaction between TXNIP and NALP3 (Fig. 9A). Our results showed that TRX activity was impeded at 48 h of HG stimulation, while it was reversed after knocking down TXNIP expression (Fig. 9B). In addition, silencing TXNIP inhibited NALP3, active caspase-1 and active IL-1β expression in cultured human podocytes under HG treatment (Fig. 9C, D). Simultaneously, being consistent with above findings, TXNIP gene silencing dramatically blocked the caspase-1 activity (Fig. 9E) and the IL-1β production (Fig. 9F) in HG-induced podocytes.

3.7. Silencing TXNIP gene alleviates HG-induced podocyte injury

Knocking down TXNIP expression suppressed desmin expression and preserved synaptopodin expression in podocytes exposed to HG for 48 h (Fig. 10A, B). HG exposure disturbed the well-defined F-actin

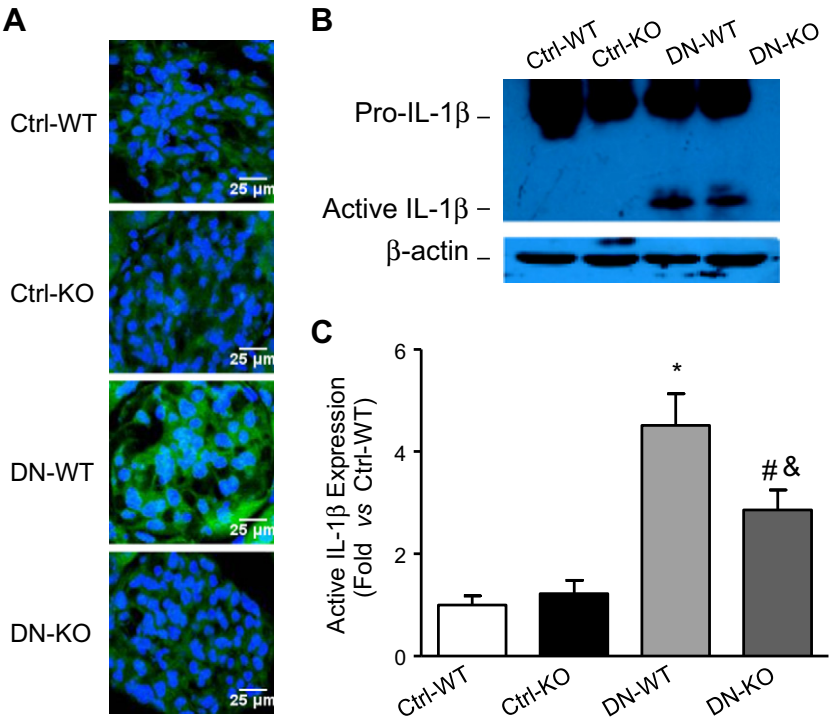

Fig. 5. Caspase-1 deficiency suppresses NALP3 inflammasome function in the glomeruli of DN mice. A. Caspase-1 activity in the glomeruli of four groups of mice by Green FLICA Caspase-1 Detection Kit. Images were representative of six images per kidney from seven mice per groups. B. Western blot analyses of IL-1β production induced by STZ in the glomerular lysate of the four groups of mice. C. Protein expression of IL-1β in the glomerular lysate of the four groups of mice (n = 6). Ctrl-WT: control wide type mice; Ctrl-KO: control caspase-1 knockout mice; DN-WT: diabetic nephropathy wide type mice; DN-KO: diabetic nephropathy caspase-1 knockout mice. $^{*}P < 0.05$ vs. Ctrl-WT; $^{\#}P < 0.05$ vs. Ctrl-KO; $^{\&}P < 0.05$ vs. DN-WT.

fibers, which exhibited normal cytoskeletal structure in control podocytes. Interestingly inhibition of TXNIP reversed this alteration (Fig. 10C, D).

4. Discussion

The purpose of the present study was to examine whether and how the NALP3 inflammasome is activated in podocytes and induces podocyte and glomerular injury in DN. Our results demonstrated that HG prompted the NALP3 inflammasome expression and activation in cultured human podocytes and in specimens derived from both human and murine models of DN. These results suggest that the NALP3 inflammasome activation may initiate podocyte injury and ultimately lead to podocyte dysfunction in DN. However, both silencing the NALP3/ASC gene and inhibiting the caspase-1 activity blocked NALP3 inflammasome activation and injury in HG-induced podocytes. These results suggest that the NALP3 inflammasome activation may be one of the major mechanisms responsible for podocyte damage under HG. Moreover, we demonstrated that TXNIP mediated the NALP3 inflammasome activation by interacting with NALP3 in podocytes.

Numerous studies have been conducted on the mechanisms of non-microbial and sterile inflammation, which have provided reasonable explanations for the pathogenesis of various renal diseases [35]. It is well known that renal inflammation and damage are mainly initiated by resident cells. Additionally, IL-1β is involved in the progression of human glomerulo-nephritis by inducing local inflammation, which is mainly produced by podocytes [17]. Moreover, the activation of NALP3 inflammasome causes the onset of non-microbial diseases including diabetes [23,36]. Activated NALP3 inflammasome subsequently prompts caspase-1 activation and initiates pro-IL-1β and pro-IL-18 cleavage into active mature forms [37]. In this regard, we hypothesized that the NALP3 inflammasome was involved in podocyte injury under HG. To test this hypothesis, our observation indicated that NALP3 inflammasome components (e.g., NALP3, ASC, and caspase-1) could colocalize with synaptopodin (the marker of podocytes) in the glomeruli of both human DN specimens and DN mice, although the intensity of synaptopodin staining decreased in the glomeruli of DN mice. The increased expression of NALP3 inflammasome components was reconfirmed in the glomeruli of DN mice by immunohistochemistry. These results suggest that the NALP3 inflammasome takes part in

Table 1
Physical and biochemical parameters of experimental animals.

Variable	Ctrl-WT	Ctrl-KO	DN-WT	DN-KO
Body weight (*g*)	23.44 ± 0.49	23.89 ± 2.29	14.70 ± 2.76*	15.93 ± 2.65**
Kw/Bw (*g/kg*)	12.65 ± 0.66	12.27 ± 1.36	19.72 ± 3.65*	16.38 ± 1.17**,***
Glucose (*mmol/l*)	5.76 ± 0.95	4.93 ± 0.61	36.25 ± 8.39*	35.91 ± 13.35**
UACR (*mg/g*)	0.73 ± 0.25	0.71 ± 0.15	25.4 ± 8.58*	17.96 ± 3.71**,***

Ctrl-WT: control wide type mice; Ctrl-KO: control caspase-1 knockout mice; DN-WT: diabetic nephropathy wide type mice; DN-KO: diabetic nephropathy caspase-1 knockout mice; Kw: kidney weight; Bw: body weight; UACR: urine albumin to creatinine ratio. Values are described as mean ± SEM for 6–8 mice in each group.
* $P < 0.0001$ vs. Ctrl-WT.
** $P < 0.0001$ vs. Ctrl-KO.
*** $P < 0.05$ vs. DN-WT.

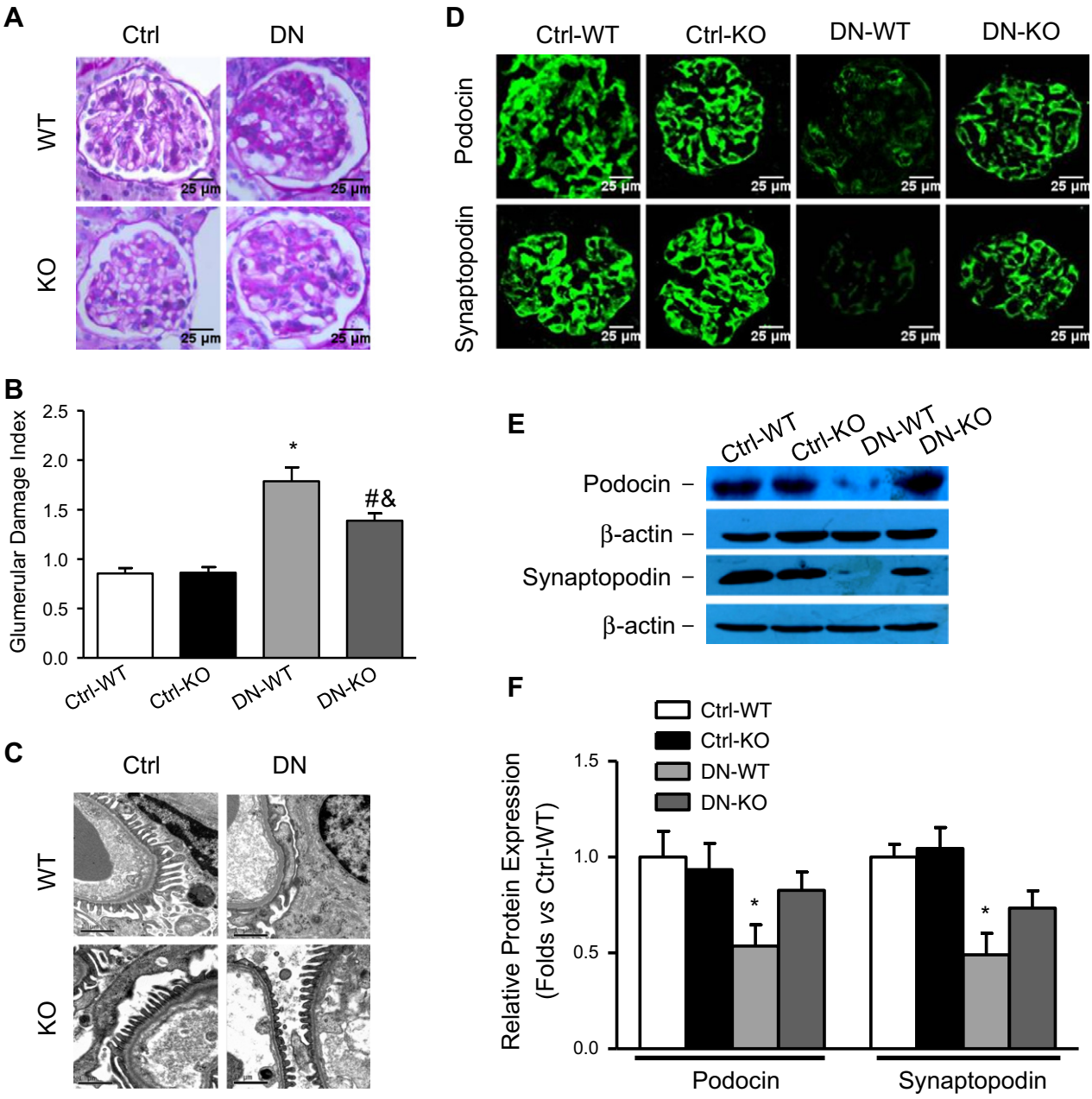

Fig. 6. Caspase-1 deficiency attenuates STZ-induced glomerular and podocyte injury in DN mice. A. PAS staining showing glomerular morphological changes. B. Summarized data of GDI by semi-quantitation of scores in the glomeruli of the four groups of mice (n = 7). For each kidney section, 50 glomeruli were randomly chosen for the calculation of GDI. C. Podocyte ultrastructure changes by TEM examination. Images were representative of six TEM images per kidney from three mice per group, bars = 1 μm. D. Immunofluorescent staining of podocin and synaptopodin in the glomeruli of the four groups of mice (n = 7). E. Western-blotting gel documents showing the expression of podocin and synaptopodin in the glomerular lysate of the four groups of mice. F. Protein expression of podocin and synaptopodin in the glomerular lysate of the four groups of mice (n = 8). Ctrl-WT: control wide type mice; Ctrl-KO: control caspase-1 knockout mice; DN-WT: diabetic nephropathy wide type mice; DN-KO: diabetic nephropathy caspase-1 knockout mice. $^{*}P < 0.05$ vs. Ctrl-WT; $^{\#}P < 0.05$ vs. Ctrl-KO; $^{\&}P < 0.05$ vs. DN-WT.

podocyte damage of DN. Furthermore, in vitro HG induced the expression and activation of NALP3 inflammasome in a time-dependent manner in cultured human podocytes. The caspase-1 activity and IL-1β production were increased simultaneously. Thus, it was proposed that HG stimulation could directly promote NALP3 inflammasome activation in podocytes.

To clarify the role of NALP3 inflammasome in podocyte injury under HG, we suppressed NALP3 inflammasome activation by shRNA or a specific inhibitor. We found that both ASC/NALP3 shRNA and inhibition of caspase-1 activity by Z-YVAD prevented caspase-1 activation and the cleavage of pro-IL-1β. As we know, IL-1β is an important proinflammatory cytokine, which controls the outcome of renal disease. In clinical trials, inhibition of IL-1β ameliorates type 2 diabetes [38]. In our present study, it was found that both silencing the ASC/NALP3 gene and inhibition of caspase-1 activity by Z-YVAD reduced the expression of desmin and rescued weakened synaptopodin expression in HG-stimulated podocytes. Desmin is a specific and sensitive indicator of the impaired podocyte [39] and its expression is usually upregulated when podocyte damage occurs [40]. Synaptopodin plays a role in adjusting the shape and movement of foot processes [41]. Collectively, these results indicated that blockade of NALP3 inflammasome activation prevented podocyte injury under HG.

Because the NALP3 inflammasome activation was involved in podocyte injury under HG and caspase-1 is a key component and

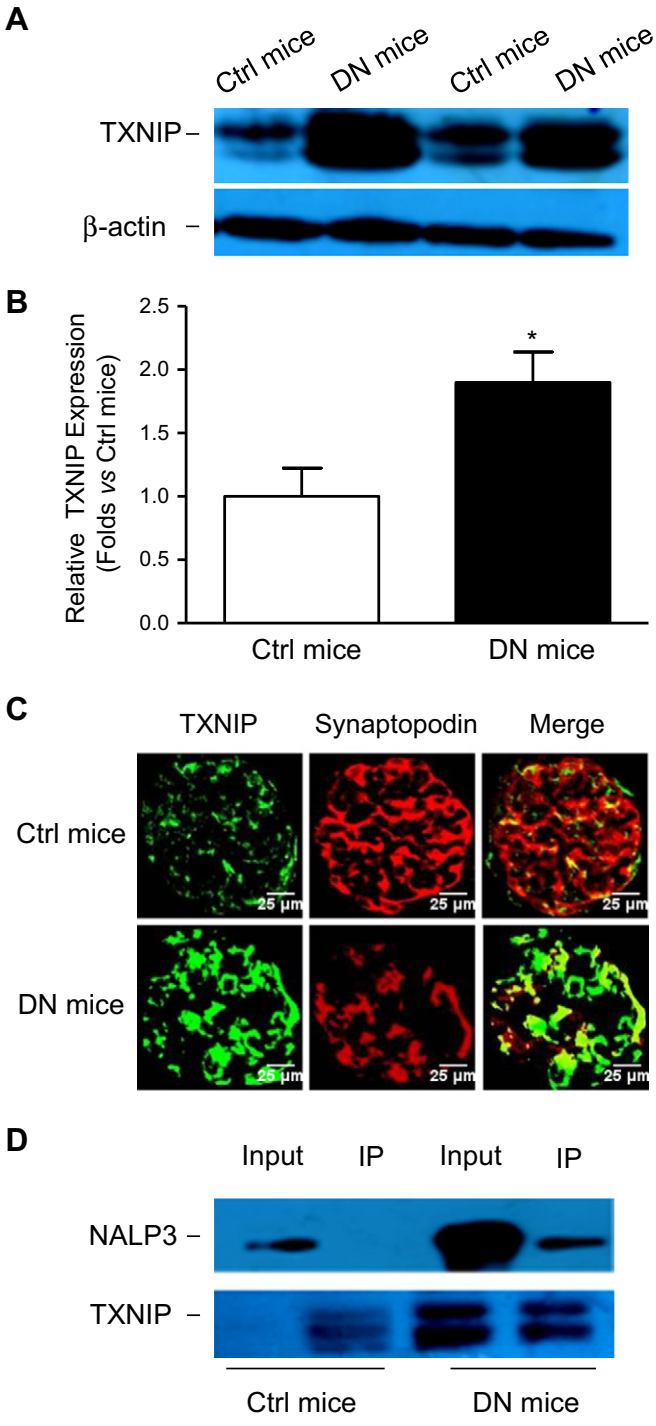

Fig. 7. TXNIP expression is upregulated in podocytes of DN mice. A. The expression of TXNIP in the glomerular lysate of both control mice and DN mice by Western blot analyses. B. Summarized data of the protein expression of TXNIP (n = 7). C. The co-localization of TXNIP with synaptopodin by confocal microscopic analysis in the glomeruli of both control mice and DN mice. D. Interaction of TXNIP with NALP3 in the glomerular lysate of both control mice and DN mice by co-immunoprecipitation. Ctrl mice:control mice; DN mice: diabetic nephropathy mice; IP: immunoprecipitation. *P < 0.05 vs. Ctrl.

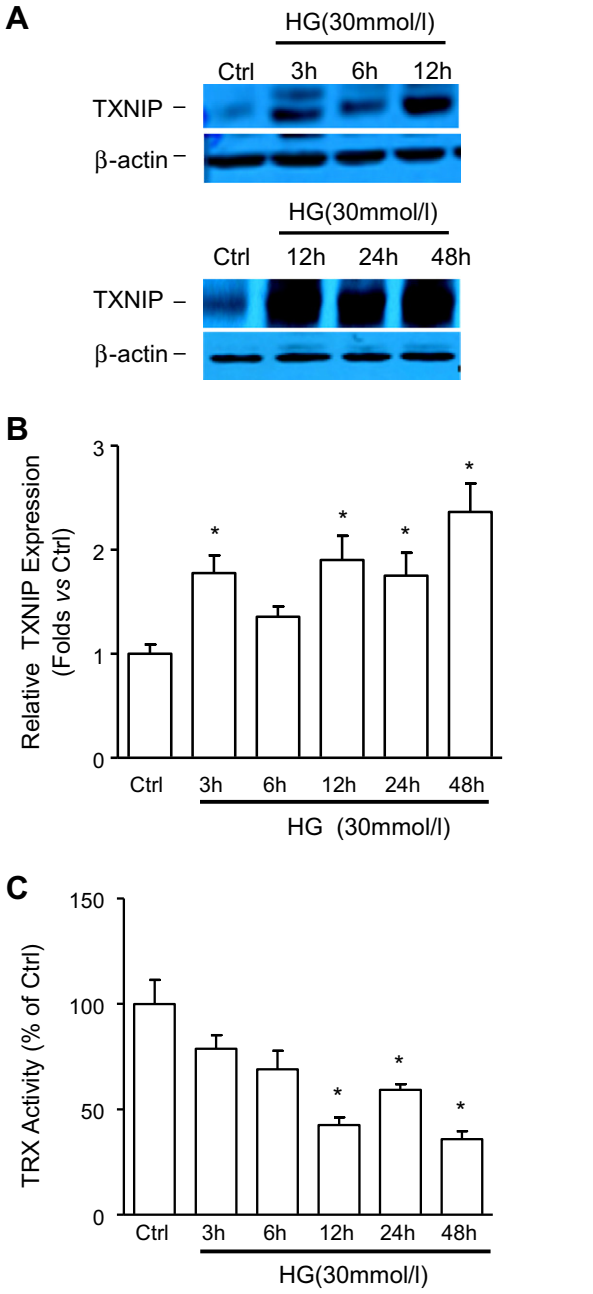

Fig. 8. HG increases the expression of TXNIP and reduces TRX activity in cultured human podocytes. A. Western-blotting gel documents showing the expression of TXNIP in cultured human podocytes by HG. B. Summarized data of TXNIP protein expression in podocytes with or without stimulation of HG (n = 6). C. TRX activity in podocytes with or without HG over time (n = 4). Ctrl:control; HG:high glucose; Veh:vehicle. *P < 0.05 vs. Ctrl.

mediator of the function of NALP3 inflammasome, we used caspase-1 KO mice to explore whether the NALP3 inflammasome activation affected the process of DN in vivo. We first found that caspase-1 deficiency reduced the cleavage of pro-IL-1β in the glomerular lysate of DN-KO mice, and then we examined its effect on glomerular and podocyte injury. The DN-KO mice exhibited a significant (i.e., 30%) reduction in urine albumin to creatinine ratio as compared with that of DN-WT mice. This implied that knocking out caspase-1 prevented renal injury in DN mice. By PAS staining, the glomerulosclerosis in DN-KO mice was evidently reduced, which further supported the view that the NALP3 inflammasome was essential for the pathogenesis of DN. It was shown for the first time that HG induced podocyte damage by triggering NALP3 inflammasome activation, which was affirmed by detecting the expression of slit diaphragm molecule podocin, and expression of the cytoskeletal molecule synaptopodin. It is also commonly appreciated that, podocin is one of the slit diaphragm complexes, and is critical for maintaining normal glomerular filtration barrier structure and function. In addition, synaptopodin has the capacity to adjust the shape and

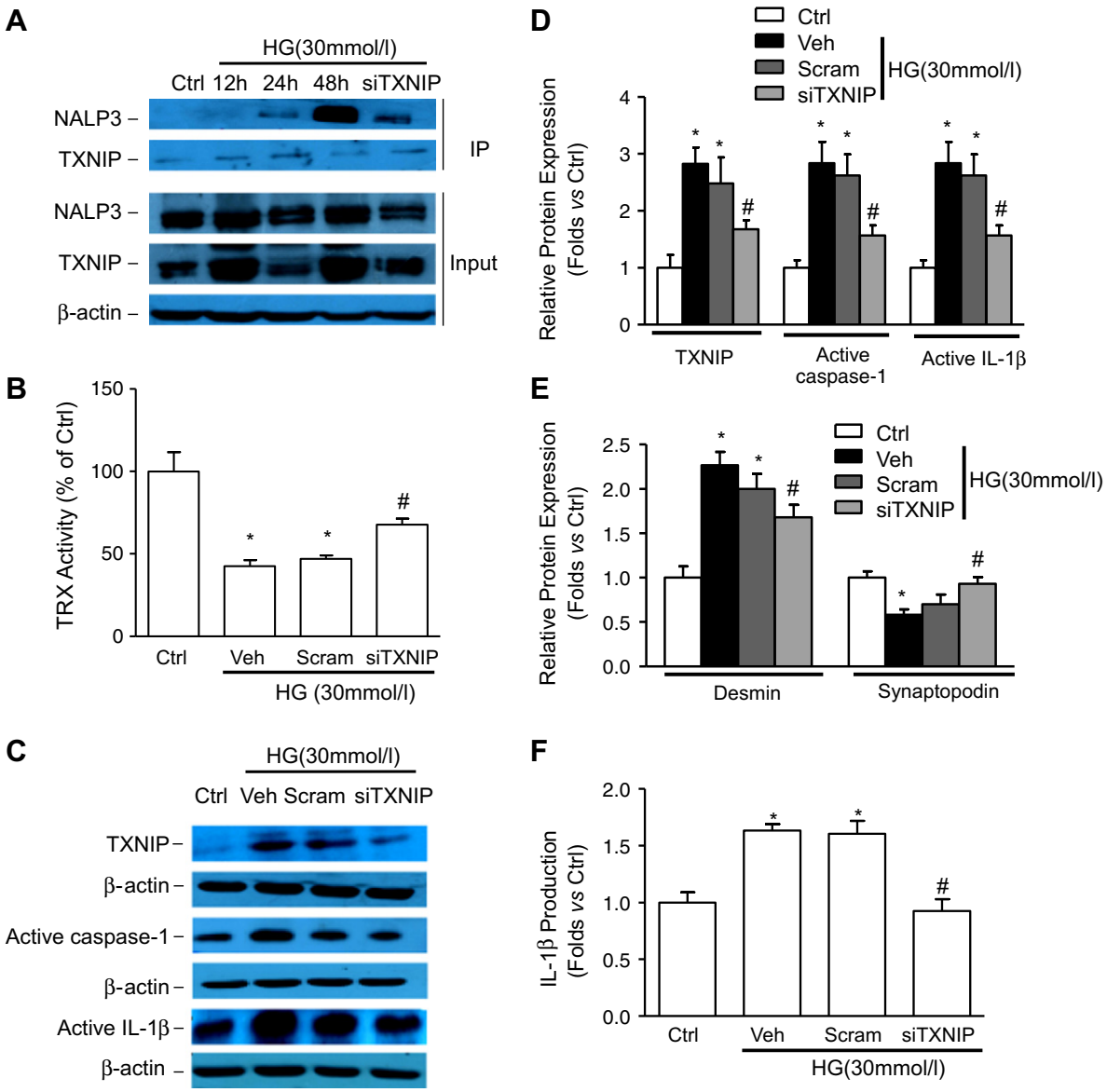

Fig. 9. Silencing TXNIP mitigates the activation of NALP3 inflammasome. A. Western blot analyses of the interaction of TXNIP with NLRP3 by co-immunoprecipitation of TXNIP in cultured human podocytes. B. TRX activity (n = 5). C. Western-blotting gel documents showing the expression of TXNIP, active caspase-1 and active IL-1β in cultured human podocytes with HG by siTXNIP. D. The protein expression of TXNIP, active caspase-1 and active IL-1β by siTXNIP (n = 5–6). E. Caspase-1 activity (n = 4). F. IL-1β production (n = 4). Ctrl:control; HG:high glucose; Veh:vehicle; Scram:scrambled siRNA; siTXNIP: TXNIP siRNA; IP:immunoprecipitation. *P < 0.05 vs. Ctrl; #P < 0.05 vs. HG.

movement of the foot processes [41]. By immunofluorescent staining and Western blotting, we demonstrated that the expression of synaptopodin and podocin in the glomeruli of DN-KO mice was higher than that of the glomeruli of DN-WT mice, which further implied that podocyte injury was markedly attenuated by caspase-1 blockade. Collectively, these observations elucidated that HG could activate NALP3 inflammasome in podocytes and glomeruli, which may be involved in the pathogenesis of early podocyte and glomerular injury during DN.

To further explore the molecular mechanism of NALP3 inflammasome activation under HG, we detected whether TXNIP mediated this process and resulted in podocyte injury. It was reported that TXNIP is an important player in the DN pathogenesis [25,42]. Zhou et al. also uncovered that TXNIP is indispensable for hyperglycemia-induced and caspase-1-dependent IL-1β production in mouse pancreatic β-cells, and that TXNIP binds with NALP3 and mediates NALP3 inflammasome activation in THP-1 cells [23].

In our study, it was found that TXNIP expression was increased in the glomerular lysate of DN mice, and the increased TXNIP was mainly distributed in podocytes of the glomeruli by confocal microscopic analysis. In addition, the interaction between TXNIP and NALP3 was strengthened in the glomerular lysate of DN mice by co-immunoprecipitation, which implied that TXNIP was involved in podocyte injury of DN by activating NALP3 inflammasome. Consistently, we elucidated that HG prompted TXNIP expression within 48 h, which reached the peak at 48 h in cultured human podocytes. By co-immunoprecipitation we also showed an increased interaction between TXNIP and NALP3 in HG-stimulated podocytes. Silencing the TXNIP gene prevented NALP3 inflammasome activation and reversed podocyte injury in HG, which was similar to the effects aroused by inhibition of NALP3/ASC. Moreover, TRX activity was gradually and time-dependently reduced within 48 h in HG-stimulated podocytes, but it was reversed after knocking down TXNIP expression. The results above inferred that TXNIP activated NALP3

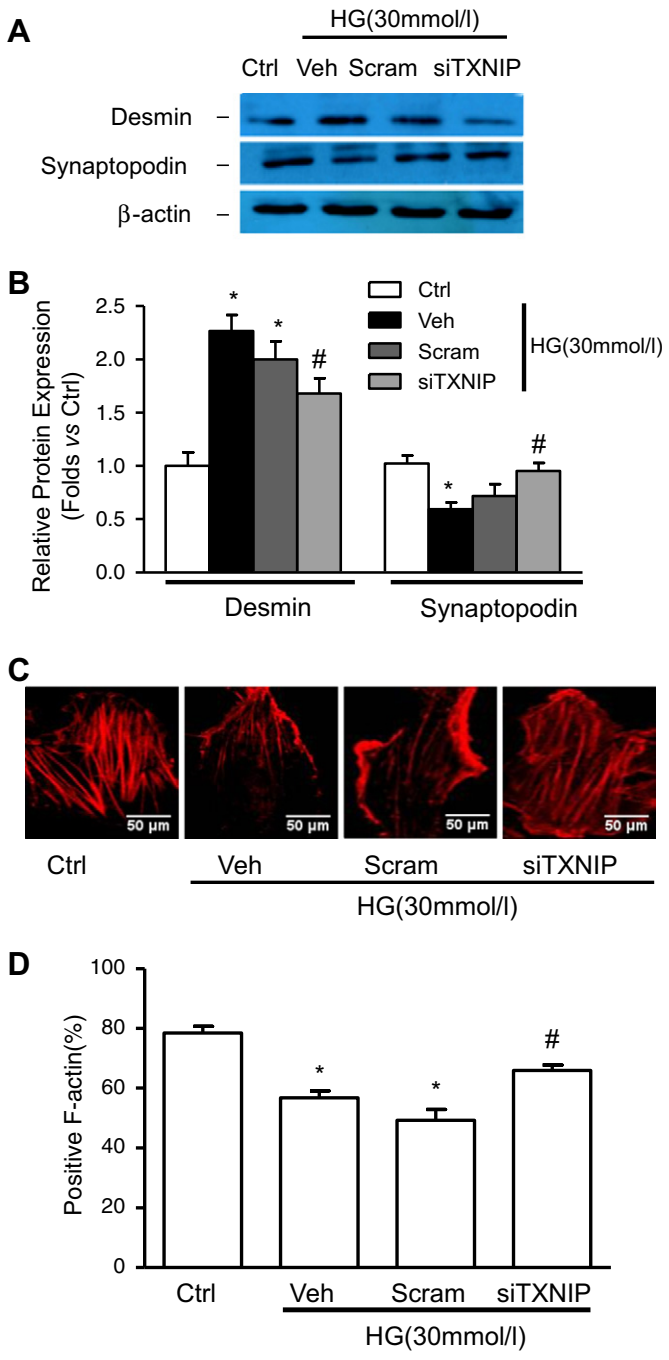

Fig. 10. Silencing TXNIP alleviates HG-induced podocyte injury. A. Western-blotting gel documents showing the effect of inhibition of TXNIP on HG-induced expression of both podocyte injury marker desmin and podocyte marker synaptopodin in cultured human podocytes. B. Protein expression of desmin and synaptopodin in cultured human podocytes ($n = 7–8$). C. Microscopic images of F-actin by rhodamine–phalloidin staining. D. Summarized data from counting the cells with distinct, longitudinal F-actin fibers. Scoring was determined from 100 podocytes on each slide ($n = 5$). Ctrl:control; HG:high glucose; Veh:vehicle; Scram:scrambled siRNA; siTXNIP: TXNIP siRNA. $^{*}P < 0.05$ vs. Ctrl; $^{\#}P < 0.05$ vs. HG.

inflammasome and in turn impaired podocyte structure and function under HG. How TXNIP mediates NALP3 inflammasome activation is an important study for us to explore in the future.

In summary, our study demonstrates that the NALP3 inflammasome is involved in podocyte injury, and the early stage of glomerular damage in DN. In addition, TXNIP can mediate NALP3 inflammasome activation and initiate IL-1β production, eventually leading to podocyte and glomerular impairment. Our current data suggest a new mechanism of podocyte injury during DN.

Acknowledgements

This work was supported by grants from the National Natural Science Foundation of China (no. 30871174, no. 81170662, no. 81170600, no. 31200872, no. 30800523, and no. 81300604), the Natural Science Foundation of Hubei Province (no. 2013 CFA026 and no. 2012 FFA038), and a Doctoral Fund obtained from the Ministry of Education of the People's Republic of China (no. 20130142110064).

References

[1] S.Y. Goh, M. Jasik, M.E. Cooper, Agents in development for the treatment of diabetic nephropathy, Expert Opin. Emerg. Drugs 13 (2008) 447–463.
[2] R.C. Atkins, P. Zimmet, Diabetic kidney disease: act now or pay later, Saudi J. Kidney Dis. Transplant. 21 (2010) 217–221.
[3] S. Dagogo-Jack, Primary prevention of type-2 diabetes in developing countries, J. Natl. Med. Assoc. 98 (2006) 415–419.
[4] A.J. Collins, R.N. Foley, B. Chavers, D. Gilbertson, C. Herzog, K. Johansen, B. Kasiske, N. Kutner, J. Liu, W. St Peter, H. Guo, S. Gustafson, B. Heubner, K. Lamb, S. Li, Y. Peng, Y. Qiu, T. Roberts, M. Skeans, J. Snyder, C. Solid, B. Thompson, C. Wang, E. Weinhandl, D. Zaun, C. Arko, S.C. Chen, F. Daniels, J. Ebben, E. Frazier, C. Hanzlik, R. Johnson, D. Sheets, X. Wang, B. Forrest, E. Constantini, S. Everson, P. Eggers, L. Agodoa, United States Renal Data System 2011 Annual Data Report: atlas of chronic kidney disease & end-stage renal disease in the United States, Am. J. Kidney Dis. 59 (2012) A7,e1-420.
[5] M. Miyauchi, M. Toyoda, K. Kobayashi, M. Abe, T. Kobayashi, M. Kato, N. Yamamoto, M. Kimura, T. Umezono, D. Suzuki, Hypertrophy and loss of podocytes in diabetic nephropathy, Intern. Med. 48 (2009) 1615–1620.
[6] S. Menini, C. Iacobini, G. Oddi, C. Ricci, P. Simonelli, S. Fallucca, M. Grattarola, F. Pugliese, C. Pesce, G. Pugliese, Increased glomerular cell (podocyte) apoptosis in rats with streptozotocin-induced diabetes mellitus: role in the development of diabetic glomerular disease, Diabetologia 50 (2007) 2591–2599.
[7] K. Reidy, K. Susztak, Epithelial-mesenchymal transition and podocyte loss in diabetic kidney disease, Am. J. Kidney Dis. 54 (2009) 590–593.
[8] Y. Yamaguchi, M. Iwano, D. Suzuki, K. Nakatani, K. Kimura, K. Harada, A. Kubo, Y. Akai, M. Toyoda, M. Kanauchi, E.G. Neilson, Y. Saito, Epithelial-mesenchymal transition as a potential explanation for podocyte depletion in diabetic nephropathy, Am. J. Kidney Dis. 54 (2009) 653–664.
[9] M.W. Steffes, D. Schmidt, R. McCrery, J.M. Basgen, Glomerular cell number in normal subjects and in type 1 diabetic patients, Kidney Int. 59 (2001) 2104–2113.
[10] M.E. Pagtalunan, P.L. Miller, S. Jumping-Eagle, R.G. Nelson, B.D. Myers, H.G. Rennke, N.S. Coplon, L. Sun, T.W. Meyer, Podocyte loss and progressive glomerular injury in type II diabetes, J. Clin. Invest. 99 (1997) 342–348.
[11] S. Mariathasan, K. Newton, D.M. Monack, D. Vucic, D.M. French, W.P. Lee, M. Roose-Girma, S. Erickson, V.M. Dixit, Differential activation of the inflammasome by caspase-1 adaptors ASC and Ipaf, Nature 430 (2004) 213–218.
[12] V. Petrilli, C. Dostert, D.A. Muruve, J. Tschopp, The inflammasome: a danger sensing complex triggering innate immunity, Curr. Opin. Immunol. 19 (2007) 615–622.
[13] S. Mariathasan, D.S. Weiss, K. Newton, J. McBride, K. O'Rourke, M. Roose-Girma, W.P. Lee, Y. Weinrauch, D.M. Monack, V.M. Dixit, Cryopyrin activates the inflammasome in response to toxins and ATP, Nature 440 (2006) 228–232.
[14] F. Martinon, A. Mayor, J. Tschopp, The inflammasomes: guardians of the body, Annu. Rev. Immunol. 27 (2009) 229–265.
[15] T.D. Kanneganti, M. Body-Malapel, A. Amer, J.H. Park, J. Whitfield, L. Franchi, Z.F. Taraporewala, D. Miller, J.T. Patton, N. Inohara, G. Nunez, Critical role for cryopyrin/Nalp3 in activation of caspase-1 in response to viral infection and double-stranded RNA, J. Biol. Chem. 281 (2006) 36560–36568.
[16] F. Martinon, V. Petrilli, A. Mayor, A. Tardivel, J. Tschopp, Gout-associated uric acid crystals activate the NALP3 inflammasome, Nature 440 (2006) 237–241.
[17] Z.I. Niemir, H. Stein, G. Dworacki, P. Mundel, N. Koehl, B. Koch, F. Autschbach, K. Andrassy, E. Ritz, R. Waldherr, H.F. Otto, Podocytes are the major source of IL-1 alpha and IL-1 beta in human glomerulonephritides, Kidney Int. 52 (1997) 393–403.
[18] S.S. Iyer, W.P. Pulskens, J.J. Sadler, L.M. Butter, G.J. Teske, T.K. Ulland, S.C. Eisenbarth, S. Florquin, R.A. Flavell, J.C. Leemans, F.S. Sutterwala, Necrotic cells trigger a sterile inflammatory response through the Nlrp3 inflammasome, Proc. Natl. Acad. Sci. U. S. A. 106 (2009) 20388–20393.
[19] C. Zhang, K.M. Boini, M. Xia, J.M. Abais, X. Li, Q. Liu, P.L. Li, Activation of Nod-like receptor protein 3 inflammasomes turns on podocyte injury and glomerular sclerosis in hyperhomocysteinemia, Hypertension 60 (2012) 154–162.
[20] A. Vilaysane, J. Chun, M.E. Seamone, W. Wang, R. Chin, S. Hirota, Y. Li, S.A. Clark, J. Tschopp, K. Trpkov, B.R. Hemmelgarn, P.L. Beck, D.A. Muruve, The NLRP3 inflammasome promotes renal inflammation and contributes to CKD, J. Am. Soc. Nephrol. 21 (2010) 1732–1744.
[21] A. Babelova, K. Moreth, W. Tsalastra-Greul, J. Zeng-Brouwers, O. Eickelberg, M.F. Young, P. Bruckner, J. Pfeilschifter, R.M. Schaefer, H.J. Grone, L. Schaefer, Biglycan, a danger signal that activates the NLRP3 inflammasome via toll-like and P2X receptors, J. Biol. Chem. 284 (2009) 24035–24048.
[22] L.K. Jones, K.M. O'Sullivan, T. Semple, M.P. Kuligowski, K. Fukami, F.Y. Ma, D.J. Nikolic-Paterson, S.R. Holdsworth, A.R. Kitching, IL-1RI deficiency ameliorates

early experimental renal interstitial fibrosis, Nephrol. Dial. Transplant. 24 (2009) 3024–3032.
[23] R. Zhou, A. Tardivel, B. Thorens, I. Choi, J. Tschopp, Thioredoxin-interacting protein links oxidative stress to inflammasome activation, Nat. Immunol. 11 (2010) 136–140.
[24] C.M. Oslowski, T. Hara, B. O'Sullivan-Murphy, K. Kanekura, S. Lu, M. Hara, S. Ishigaki, L.J. Zhu, E. Hayashi, S.T. Hui, D. Greiner, R.J. Kaufman, R. Bortell, F. Urano, Thioredoxin-interacting protein mediates ER stress-induced beta cell death through initiation of the inflammasome, Cell Metab. 16 (2012) 265–273.
[25] A. Advani, R.E. Gilbert, K. Thai, R.M. Gow, R.G. Langham, A.J. Cox, K.A. Connelly, Y. Zhang, A.M. Herzenberg, P.K. Christensen, C.A. Pollock, W. Qi, S.M. Tan, H.H. Parving, D.J. Kelly, Expression, localization, and function of the thioredoxin system in diabetic nephropathy, J. Am. Soc. Nephrol. 20 (2009) 730–741.
[26] A.M. Kaimul, H. Nakamura, H. Masutani, J. Yodoi, Thioredoxin and thioredoxin-binding protein-2 in cancer and metabolic syndrome, Free Radic. Biol. Med. 43 (2007) 861–868.
[27] K. Schroder, R. Zhou, J. Tschopp, The NLRP3 inflammasome: a sensor for metabolic danger? Science 327 (2010) 296–300.
[28] J. Chen, G. Saxena, I.N. Mungrue, A.J. Lusis, A. Shalev, Thioredoxin-interacting protein: a critical link between glucose toxicity and beta-cell apoptosis, Diabetes 57 (2008) 938–944.
[29] B.C. Liu, X. Song, X.Y. Lu, D.T. Li, D.C. Eaton, B.Z. Shen, X.Q. Li, H.P. Ma, High glucose induces podocyte apoptosis by stimulating TRPC6 via elevation of reactive oxygen species, Biochim. Biophys. Acta 1833 (2013) 1434–1442.
[30] F.F. He, C. Zhang, S. Chen, B.Q. Deng, H. Wang, N. Shao, X.J. Tian, Z. Fang, X.F. Sun, J.S. Liu, Z.H. Zhu, X.F. Meng, Role of CD2-associated protein in albumin overload-induced apoptosis in podocytes, Cell Biol. Int. 35 (2011) 827–834.
[31] C. Zhang, J.J. Hu, M. Xia, K.M. Boini, C.A. Brimson, L.A. Laperle, P.L. Li, Protection of podocytes from hyperhomocysteinemia-induced injury by deletion of the gp91phox gene, Free Radic. Biol. Med. 48 (2010) 1109–1117.
[32] J. Toyonaga, K. Tsuruya, H. Ikeda, H. Noguchi, H. Yotsueda, K. Fujisaki, M. Hirakawa, M. Taniguchi, K. Masutani, M. Iida, Spironolactone inhibits hyperglycemia-induced podocyte injury by attenuating ROS production, Nephrol. Dial. Transplant. 26 (2011) 2475–2484.
[33] E. Junn, S.H. Han, J.Y. Im, Y. Yang, E.W. Cho, H.D. Um, D.K. Kim, K.W. Lee, P.L. Han, S.G. Rhee, I. Choi, Vitamin D3 up-regulated protein 1 mediates oxidative stress via suppressing the thioredoxin function, J. Immunol. 164 (2000) 6287–6295.
[34] A. Nishiyama, M. Matsui, S. Iwata, K. Hirota, H. Masutani, H. Nakamura, Y. Takagi, H. Sono, Y. Gon, J. Yodoi, Identification of thioredoxin-binding protein-2/vitamin D(3) up-regulated protein 1 as a negative regulator of thioredoxin function and expression, J. Biol. Chem. 274 (1999) 21645–21650.
[35] M. Segelmark, T. Hellmark, Autoimmune kidney diseases, Autoimmun. Rev. 9 (2010) A366–A371.
[36] S.L. Cassel, F.S. Sutterwala, Sterile inflammatory responses mediated by the NLRP3 inflammasome, Eur. J. Immunol. 40 (2010) 607–611.
[37] F. Martinon, K. Burns, J. Tschopp, The inflammasome: a molecular platform triggering activation of inflammatory caspases and processing of proIL-beta, Mol. Cell 10 (2002) 417–426.
[38] C.M. Larsen, M. Faulenbach, A. Vaag, A. Volund, J.A. Ehses, B. Seifert, T. Mandrup-Poulsen, M.Y. Donath, Interleukin-1-receptor antagonist in type 2 diabetes mellitus, N. Engl. J. Med. 356 (2007) 1517–1526.
[39] U. Sen, P. Basu, O.A. Abe, S. Givvimani, N. Tyagi, N. Metreveli, K.S. Shah, J.C. Passmore, S.C. Tyagi, Hydrogen sulfide ameliorates hyperhomocysteinemia-associated chronic renal failure, Am. J. Physiol. Ren. Physiol. 297 (2009) F410–F419.
[40] J. Zou, E. Yaoita, Y. Watanabe, Y. Yoshida, M. Nameta, H. Li, Z. Qu, T. Yamamoto, Upregulation of nestin, vimentin, and desmin in rat podocytes in response to injury, Virchows Arch. 448 (2006) 485–492.
[41] P. Mundel, H.W. Heid, T.M. Mundel, M. Kruger, J. Reiser, W. Kriz, Synaptopodin: an actin-associated protein in telencephalic dendrites and renal podocytes, J. Cell Biol. 139 (1997) 193–204.
[42] Y. Hamada, M. Fukagawa, A possible role of thioredoxin interacting protein in the pathogenesis of streptozotocin-induced diabetic nephropathy, Kobe J. Med. Sci. 53 (2007) 53–61.